

# Generation of parabolic bound pulses from a Yb-fiber laser

**B. Ortaç\*, A. Hideur, M. Brunel, C. Chédot**

*Groupe d'Optique et d'Optronique, UMR 6614 CORIA, Université de Rouen, Avenue de l'université BP 12, 76801 Saint Etienne du Rouvray Cedex, France*

*\*Present address: Friedrich-Schiller University, Institute of applied physics, Albert-Einstein Str.15, 07745 Jena, Germany*  
[ortac@iap.uni-jena.de](mailto:ortac@iap.uni-jena.de)

**J. Limpert, A. Tünnermann**

*Friedrich-Schiller University, Institute of applied physics, Albert-Einstein Str.15, 07745 Jena, Germany*

**F. Ö. Ilday**

*Department of Physics, Bilkent University, Ankara, 06800 Turkey*

**Abstract:** We report the observation of self-similar propagation of bound-state pulses in an ytterbium-doped double-clad fiber laser. A bound state of two positively chirped parabolic pulses with 5.4 ps duration separated by 14.9 ps is obtained, with 1.7 nJ of energy per pulse. These pulses are extra-cavity compressed to 100 fs. For higher pumping power and a different setting of the intra-cavity polarization controllers, the laser generates a bound state of three chirped parabolic pulses with different time separations and more than 1.5 nJ energy per pulse. Perturbation of this bound state by decreasing pump power results in the generation of a single pulse and a two-pulse bound state both structures traveling at the same velocity along the cavity. A possible explanation of the zero relative speed by a particular phase relation of the bound states is discussed.

©2006 Optical Society of America

**OCIS codes:** (140.3510) Lasers, fiber; (140.7090) Ultrafast lasers; (060.4370) Nonlinear optics

---

## References and links

1. H. A. Haus, K. Tamura, L. E. Nelson, and E. P. Ippen, "Stretched-pulse additive-pulse mode-locking in fiber ring lasers : theory and experiment," *IEEE J. Quantum. Electron.* **31**, 591-598 (1995).
2. F. Ö. Ilday, J. Buckley, L. Kuznetsova, and F. W. Wise, "Generation of 36-femtosecond pulses from a ytterbium fiber laser," *Opt. Express* **11**, 3550-3554 (2003).
3. H. Lim, F. Ö. Ilday, and F. W. Wise, "Generation of 2 nJ pulses from a femtosecond ytterbium fiber laser," *Opt. Lett.* **28**, 660-662 (2003).
4. K. Tamura, L. E. Nelson, H. A. Haus, E. P. Ippen, "Soliton versus nonsoliton operation of fiber ring lasers," *Appl. Phys. Lett.* **64**, 149 (1994).
5. G. Lenz, K. Tamura, H. A. Haus, and E. P. Ippen, "All-solid-state femtosecond source at 1.55  $\mu\text{m}$ ," *Opt. Lett.* **20**, 1289-1291 (1995).
6. M. Olivier, V. Roy, M. Piché, F. Babin, "Pulse collision in the stretched-pulse fiber lasers," *Opt. Lett.* **29**, 1461-1463 (2004).
7. F. Ö. Ilday, J. R. Buckley, H. Lim, F. W. Wise, W. G. Clark, "Generation of 50-fs, 5-nJ pulses at 1.03  $\mu\text{m}$  from a wave-breaking-free fiber laser," *Opt. Lett.* **28**, 1365-1367 (2003).
8. R.P. Davey, N. Langford, A.I. Ferguson, "Interacting solutions in erbium fibre laser," *Electron. Lett.* **27**, 1257 (1991)
9. D.J. Richardson, R.I. Laming, D.N. Payne, V.J. Matsas, N.W. Phillips, "Pulse repetition rates in passive, selfstarting, femtosecond soliton fibre laser," *Electron. Lett.* **27**, 1451 (1991).

10. B. Ortaç, A. Hideur, M. Brunel, "Passive harmonic mode locking with a high-power ytterbium-doped double-clad fiber laser," *Opt. Lett.* **29**, 1995 (2004).
11. Y. Deng, W. H. Knox, "Self-starting passively harmonic mode-locked femtosecond Yb<sup>3+</sup>-doped fiber laser at 1030 nm," *Opt. Lett.* **29**, 2121 (2004).
12. A. Hideur, B. Ortaç, T. Chartier, M. Brunel, H. Leblond and F. Sanchez, "Ultra-short bound states generation with a passively mode-locked high-power Yb-doped double-clad fiber laser," *Opt. Commun.* **225**, 71 (2003).
13. D. Y. Tang, B. Zhao, D. Y. Shen, C. Lu, W. S. Man, and H. Y. Tam, "Bound-soliton fiber laser," *Phys. Rev. A* **66**, 033806 (2002).
14. Ph. Grelu, F. Belhache, F. Guty, and J. M. Soto-Crespo, "Phase-locked soliton pairs in a stretched-pulse fiber laser," *Opt. Lett.* **27**, 966 (2002).
15. P. Grelu, J. Béal, and J. M. Soto-Crespo, "Soliton pairs in a fiber laser: from anomalous to normal average dispersion regime," *Opt. Express* **11**, 2238-2243 (2003).
16. J. M. Soto-Crespo, N. Akhmediev, Ph. Grelu and F. Belhache, "Quantized separations of phase-locked soliton pairs in fiber lasers," *Opt. Lett.* **28**, 1757-1759 (2003).
17. B. Ortaç, A. Hideur, T. Chartier, M. Brunel, Ph. Grelu, H. Leblond and F. Sanchez, "Generation of bound states of three ultra-short pulses with a passively mode-locked high-power Yb-doped double-clad fiber laser," *IEEE Photon. Technol. Lett.* **16**, 1274-1276 (2004).
18. B. Ortaç, A. Hideur, M. Brunel, "Binding widely separated pulses with a passively mode-locked high-power Yb-doped double-clad fiber laser," *Appl. Phys. B* **79**, 185 (2004).
19. F. O. Ilday, J. R. Buckley, W. G. Clark and F. W. Wise, "Self similar evolution of parabolic pulses in a laser," *Phys. Rev. Lett.* **92**, 213902 (2004).
20. J. R. Buckley, F. W. Wise, F. Ö. Ilday, T. Sosnowski, "Femtosecond fiber lasers with pulse energies above 10 nJ," *Opt. Lett.* **30**, 1888-1890 (2005).
21. B. Ortaç, A. Hideur, T. Chartier, M. Brunel, C. Özkul, F. Sanchez, "90 fs generation from a stretched-pulse ytterbium doped fiber laser," *Opt. Lett.* **28**, 1305 (2003).
22. B. Ortaç, A. Hideur, C. Chedot, M. Brunel, G. Martel, and J. Limpert, "Self-similar low-noise ytterbium-doped double-clad fiber laser," submitted to *Appl. Phys. B*.
23. M. Olivier, V. Roy, M. Piché, and F. Babin, "Pulse collisions in the stretched-pulse fiber laser," *Opt. Lett.* **29**, 1461-1463 (2004).
24. P. Grelu and N. Akhmediev, "Group interactions of dissipative solitons in a laser cavity: the case of 2+1," *Opt. Express* **12**, 3184-3189 (2004).
25. V. Roy, M. Olivier, F. Babin, and Michel Piché, "Dynamics of periodic pulse collisions in strongly dissipative-dispersive system," *Phys. Rev. Lett.* **94**, 203903 (2005).
26. N. Akhmediev, J. M. Soto-Crespo, M. Grapinet, Ph. Grelu, "Dissipative soliton interaction inside a fiber laser cavity," *Opt. F. Technol.* **11**, 209-228 (2005).
27. V. Roy, M. Olivier, and M. Piché, "Pulse interactions in the stretched-pulse fiber laser," *Opt. Express* **13**, 9217-9223 (2005).

## 1. Introduction

Ytterbium-doped fiber lasers have attracted much interest in the last few years as sources of femtosecond pulses due to the large gain bandwidth and exceptional efficiency of ytterbium-doped fibers, as well as the convenience of pumping with telecom-grade laser diodes. The association of these characteristics with the high stability, compact size and efficient heat dissipation of fiber technology make these lasers practical alternatives to bulk laser systems. To date, the shortest and most energetic pulses generated in a fiber laser are obtained using polarization additive pulse mode-locking (P-APM) [1]. In particular, using intracavity dispersion management, it is possible to produce pulses with durations as short as 36 fs and energies as high as 2 nJ [2,3]. This stretched-pulse laser configuration can support higher energies than conventional soliton fiber lasers [4]. Nevertheless, they are limited to less than 3 nJ by the saturation of the P-APM mechanism [5,6] and wave-breaking in the anomalous dispersion fiber segment [7]. As a consequence, the laser operates in multiple pulsing mode, i.e., several pulses coexist in the cavity, when the pump power is increased beyond a critical value [8,9]. In soliton fiber lasers, this behavior is observed at a lower threshold due to soliton energy quantization [8]. In general, these pulses are randomly separated. Under certain conditions these pulses can be regularly spaced in the cavity leading to passive harmonic

mode-locking [10,11]. The existence of multiple pulses can also lead to bound states of closely spaced pulses [12]. These regimes of emission have been intensively investigated in low-power erbium-doped fiber lasers in the normal- and anomalous averaged cavity dispersion [13-16]. In the soliton regime, it has been shown that bound states arise from the nonlinear interaction between solitons and resonant dispersive waves. These are latter emitted as a result of the periodic perturbations the solitons undergo along the laser cavity on successive round trips [16]. In the stretched-pulse regime, the resonant sidebands are strongly reduced because of the alternating broadening and compression the pulse experience in single cavity roundtrip [1]. Nevertheless, direct interaction is more significant since the stretched pulses in a pulse bound state present a strong overlap in a sizeable portion of the laser cavity [15]. Recent experiments on ytterbium fiber lasers operating in the normal dispersion regime have shown that high-energetic bound states of two or three femtosecond pulses with temporal separations ranging from a few picoseconds to more than 150 ps can be generated [12,17,18].

Ilday *et al.* have recently demonstrated a new regime of mode-locking: wave-breaking is suppressed by exploiting self-similar pulse propagation, which is resistant to nonlinearity [7,19,20]. Femtosecond pulses with more than 10 nJ energy have already been generated [19] and theoretical predictions promote the possibility of some hundreds of nanojoules [18]. However, a less fundamental, but a stringent limitation to the pulse energy arises from overdriving of the P-APM mechanism, which results in multiple-pulsing at high pumping powers [19]. Therefore, it is important to understand the mechanisms of multiple pulsing, including bound pulse formation, both for the practical goal of generating pulses with higher energies and for a fuller understanding of mode-locked laser dynamics.

Here, we report, for the first time to our knowledge, the observation of bound states of two and three parabolic pulses in an ytterbium-doped fiber laser operating in the self-similar regime. Consequently, this ubiquitous phenomenon is confirmed to exist in all fiber lasers utilizing the P-APM mechanism, whether the laser operates in the soliton, stretched-pulse, or self-similar regimes.

## 2. Experimental setup

The experimental setup consists of a fiber laser utilizing P-APM (Fig. 1) [1, 21]. A polarizing isolator provides unidirectional operation and polarization selectivity in a ring-cavity configuration. The amplifying medium is a double-clad ytterbium-doped fiber, which is side-pumped using the v-groove technique by a large strip diode with a maximum power of 3.7 W at 975 nm. The single-mode core diameter of the double-clad gain fiber is 7  $\mu\text{m}$  with a numerical aperture of 0.12 and its second cladding is a 125x125  $\mu\text{m}^2$  square with a numerical aperture of 0.4. The length of the gain fiber is 4 m, which allows nearly complete absorption of the pump power. Undoped single-mode fibers are spliced to both ends of the double-clad gain fiber leading to a total fiber length of about 8 m. The free-space section of the cavity is about 1 m-long. The average group-velocity dispersion of the gain fiber and the undoped fibers has been measured using the sideband method to be 0.026 ps<sup>2</sup>/m around 1050 nm. A grating pair with 1200 lines/mm partially compensates the positive (normal) group-velocity dispersion of the fiber. All the results presented below are obtained for an overall grating separation of 2.2 cm, which corresponds to a second order GVD of -0.16 ps<sup>2</sup> at 1050 nm. The total cavity GVD is then +0.047 ps<sup>2</sup>. The zero-order diffraction of the first grating serves as the output coupler, and a half-wave plate introduced right after the isolator allows precise control of the output coupling ratio.

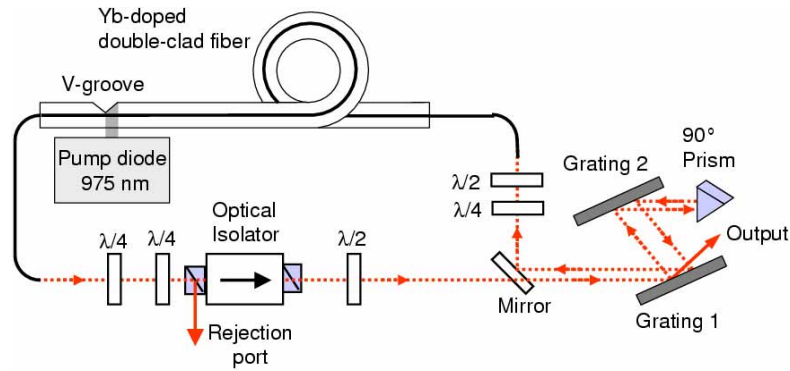


Fig. 1. Experimental setup.

### 3. Results

#### 3.1 Bound states of two parabolic pulses

The operation of the laser is strongly dependent on the orientation of the intra-cavity polarization controllers. Generation of highly energetic and ultra-short bound states of two stretched-pulses has been reported in Ref 12. Here we are interested in the generation of bound states of parabolic pulses. Typical operation of this laser in the single pulse regime is obtained for about 1.7 W pump power and chirped-parabolic pulses with 6.5 ps duration and 3.2 nJ energy are then generated [22]. The orientation of the wave plates is intentionally chosen such that the laser generates two bound parabolic pulses. The output-coupling coefficient is relatively high (about 75 %). The pump-power threshold leading to this regime corresponds to a pump power of 1.8 W. The fundamental cavity repetition rate is 20 MHz. Fig. 2(a) shows the optical power spectrum of the bound pulses. The optical spectrum is modulated by a two-wave interference pattern with a contrast approaching unity as shown on the expanded portion of the spectrum in the inset of Fig. 2(a). This high-contrast interference pattern remains stable for hours indicating that the two pulses comprising the bound-pulse have a fixed phase relationship. The period of the spectral modulation is  $\Delta\lambda = 0.25$  nm, which implies a pulse separation of  $\Delta\tau = 14.9$  ps. The autocorrelation trace shown in Fig. 2(b) confirms this separation, with the two side-peaks situated at 14.9 ps from the central peak. Given that the secondary peaks of the autocorrelation trace are half of the main peak, we infer that the two pulses are equal in size. Fig. 2(b) shows also theoretical fits of the central peak with  $\text{sech}^2$ , Gaussian and parabolic profiles. The experimental autocorrelation shows better agreement with a parabolic pulse profile, which is consistent with self-similar pulse propagation. This assumption is supported by the observation of the optical spectrum. This is reflected in the spectrum, which exhibits a parabolic shape around the center with a transition to a steep decay (see Fig. 2(a)). In Fig. 2(a), the spectral width is best fit with a 26 nm parabolic shape centered around 1052 nm. The pulse duration assuming a parabolic pulse shape is 5.45 ps. The pulse pair can be compressed extra-cavity using a grating pair. The best fit is obtained with a  $\text{sech}^2$  profile leading to a pulse duration of 115 fs (see Fig. 3).

The correct spectral shape (parabolic around the center with a transition to a steep decay) is a necessary condition but not sufficient to conclude about the self-similar propagation of the pulses inside the cavity. Indeed, such parabolic profile could be obtained while the pulse propagation remain consistent with a stretched-pulse evolution which is characterized by two minima of the pulse duration inside the cavity [1]. Results corresponding to such situations have been already reported in references 12, 17 and 18. Moreover, the transition from the stretched-pulse regime to the self-similar propagation regime is obtained by changing the setting of the intra-cavity polarization controllers while maintaining fixed all the other

parameters (average cavity dispersion, pumping power, and output coupling). So, the distinction between these two regimes must be clearly defined using other criteria.

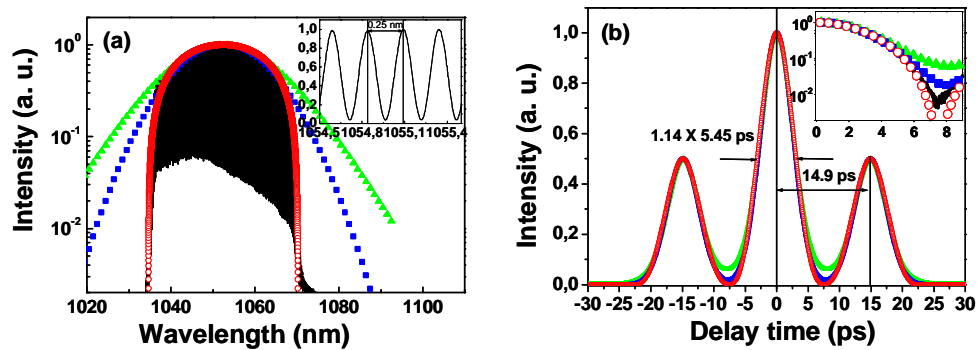


Fig. 2. (a) Optical spectrum of the twin pulses in the bound state. The spectrum is fit with parabolic (open circles), Gaussian (closed squares), and  $\text{sech}^2$  (closed triangles) pulse shapes. The inset shows a zoomed-in portion of the optical spectrum on a linear scale. (b) Second-order intensity autocorrelation trace of the two bound parabolic pulses observed directly at the laser output. The theoretical fits with parabolic (open circles), Gaussian (closed square curves) and  $\text{sech}^2$  (closed triangle curves) pulse shapes are also shown. Inset shows detail of the autocorrelation trace on a logarithmic scale.

The second important requirement for self similar pulse propagation in an oscillator rise from the particular evolution of the pulse as it traverses the laser which is fundamentally distinct from the pulse evolution in soliton and stretched-pulse lasers. The pulse is always positively chirped inside the laser with a minimum pulse duration after the intra-cavity gratings just before entering the fiber [18-19]. Information about the intra-cavity pulse evolution could be inferred from the magnitude of anomalous GVD required to dechirp the pulse pair outside the cavity. In our case, the anomalous dispersion necessary for compression of the parabolic pulses is approximately  $0.20 \text{ ps}^2$ , whereas the intra-cavity grating pair provides  $0.16 \text{ ps}^2$ . This indicates that the pulses are still highly positively chirped before entering the fiber after the intra-cavity gratings. Therefore, we conclude that the pulses are always positively chirped inside the cavity with a minimum near the beginning of the fiber just after the gratings.

We measured 70 mW average output power for a pump power of 1.8 W which corresponds to 1.75 nJ energy per pulse. For the output-coupling ratio of 75%, the estimated intra-cavity pulse energy is 2.3 nJ. The extracted pulse energy is lower than that obtained in the stretched pulse regime [12]. It is natural to ask why energy is weaker in our case whereas the results reported on similariton lasers show that this regime of operation is favorable for high energy extraction from fiber oscillators [18-19]. We believe that limitation of pulse energy in our case could be attributed to the large length of gain fiber used in our configuration. As a consequence, nonlinearities experienced by the pulse during amplification are very important leading to the saturation of the P-APM mechanism at low energy levels. This suggests that to benefit maximally from the similariton regime, it is essential to design an adequate cavity for nonlinearity management.

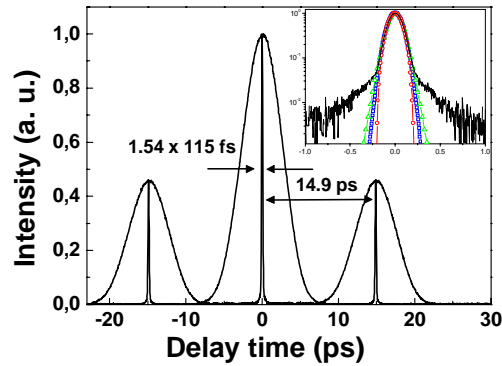


Fig. 3. Autocorrelation trace of the dechirped (solid line) and chirped (dashed line) twin bound state pulses. Inset shows the central peak of the autocorrelation trace after extra-cavity dechirping on a logarithmic scale. The theoretical fits with parabolic (open circles), Gaussian (closed square curves) and  $\text{sech}^2$  (closed triangle curves) pulse shapes are also shown on the inset. Pulse duration assuming a  $\text{sech}^2$  shape is 115 fs.

### 3.2 Bound states of three parabolic pulses

It is natural to expect that multiple bound pulses should be observed at higher powers. Indeed, at higher pump power and for a different setting of the polarization controllers, we observe the emission of bound states of three parabolic pulses with different time delays. The scenario leading to the formation of this bound state is as follows. The output coupling is maintained at the high value of 75%. At the lowest pump powers, only continuous wave (cw) operation is observed. The mode-locking threshold is reached at a pump power of 1.9 W, at which point the laser directly exhibits a bound state of three parabolic pulses. Fig. 4 shows the corresponding optical spectrum, as well as theoretical fits by  $\text{sech}^2$ , Gaussian and parabolic profiles. The spectrum is strongly modulated, which indicates that a precise phase relationship is maintained between the pulses; modulation contrast approaches unity over the entire 30 nm spectral width. A magnified portion of this spectrum is shown in the inset of Fig. 4. The alternation of higher and lower intensity fringes is typical of three-wave interference. In addition, the overmodulation of the fringes indicates that the laser generates three pulses with different time separations. By Fourier-transforming this spectrum, its modulation was checked to be compatible with three identical pulses having two different but close separations. The measured autocorrelation traces obtained before and after pulse dechirping are presented in Fig. 5. It results effectively from the existence of three pulses with equal amplitudes but with two different time separations  $\Delta\tau_1$  and  $\Delta\tau_2$ , providing seven peaks in ratio 1/3, 1/3, 1/3, 1, 1/3, 1/3, 1/3. From the autocorrelation trace, we can deduce that the time separations between adjacent pulses are  $\Delta\tau_1=18.13$  ps and  $\Delta\tau_2=19.97$  ps, which correspond to the different "pseudo-periods" of the spectral modulation deduced from the zoom of the spectrum (inset in Fig. 4). The optical spectrum is best fit with a parabolic profile with a spectral width of about 30 nm (Fig. 4). The inset of Fig. 5 shows the details of the central peak of the chirped pulses autocorrelation trace. The chirped pulses are fit well with a parabolic profile over more than one order of intensity variation, consistent with self-similar pulse formation. The chirped pulses duration is 5.9 ps. It is about 10% longer than in the case of the twin pulse regime. These pulses are extra-cavity compressed to 100 fs, assuming  $\text{sech}^2$  shape. We measure an output power of 95 mW for 1.9 W of pump power. The energy content of each pulse is, thus, estimated to be 1.6 nJ (2.13 nJ intra-cavity). It was confirmed that in this case as well the negative dispersion needed for external compression is higher than that provided by the intra-cavity grating pair.

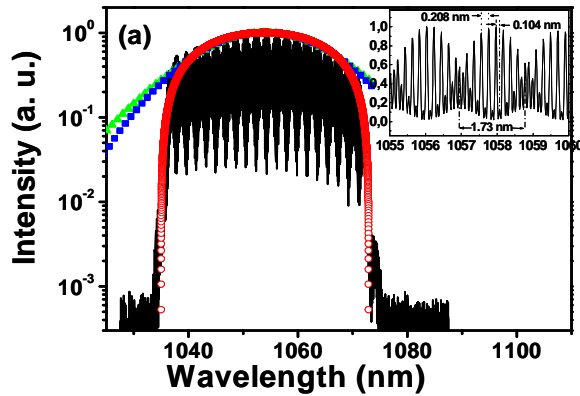


Fig. 4. Optical spectrum of the triplet featuring different separations. The spectrum is fit with parabolic (open circles), Gaussian (closed squares), and  $\text{sech}^2$  (closed triangles) pulse shapes. The inset shows a magnified portion of the optical spectrum on linear scale.

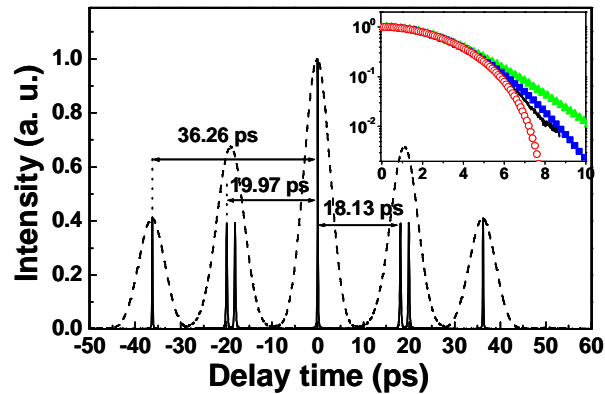


Fig. 5. Autocorrelation trace of the chirped (dashed line) and dechirped (solid line) triplet bound state featuring different separations. Inset shows the central peak of the autocorrelation trace with theoretical fits for parabolic (open circles), Gaussian (closed squares) and  $\text{sech}^2$  (closed triangles).

It is common for highly nonlinear, mode-locked lasers to exhibit strong hysteresis between mode-locking and cw operation. In the presence of the three bound pulses, by decreasing the pump power to 1.85 W, while keeping all other parameters unchanged, we observe the disassociation of the third pulse from the bound triplet state: stable co-emission of a pair of bound parabolic pulses coexists with a single parabolic pulse within the same cavity round trip. We thus obtain a bound state of two parabolic pulses and a single parabolic pulse, separated by 22 ns. The temporal trace observed with a 5-GHz oscilloscope and an 8-GHz photodetector is presented in Fig. 6(a). The oscilloscope traces feature two peaks per cavity roundtrip. The largest one, identified as a doublet, is twice the second one in amplitude which is identified as a singlet. The two peaks appear stably on the screen and do not collide together. Note that the cavity roundtrip time is 50 ns.

Pulse collisions in fiber lasers have recently attracted much interest and different interaction scenarios have been reported [22-26]. Collisions can take place between a bound state of two or more pulses and a single pulse. In particular, the interaction of a two pulses bound state and a single pulse have been largely studied [22-26]. The interaction process is a result of the asymmetry of the bound state because of the  $\pi/2$  phase difference between the

two pulses. Hence, the doublet and the singlet move at different velocities leading to their collision at some stage in the cavity [26]. This process can repeat itself indefinitely with relatively long period.

The absence of collision between the singlet and the doublet generated in our case means that both structures move endlessly at the same group velocity. This zero relative speed could be related to the fact that the phase difference between the two pulses of the pair is zero or  $\pi$ . Note that such phase relationships have been theoretically predicted in the case of an erbium doped fiber laser operating in the normal dispersion regime [15]. Unfortunately, the phase relationship between the two pulses of the doublet could not be inferred from the position of the fringes because of their large time separation (more than 315 times the dechirped pulse duration). Numerical simulations are clearly needed to understand the key parameters underlying the self-similar bound pulses operation and give more precisions about their phase relationship characteristic. Fig. 6(b) shows the corresponding optical spectrum with three different theoretical fits. The optical spectrum is best fit with a 29-nm wide parabolic profile. The spectrum is modulated with a two-wave interference pattern, and the modulation contrast is diminished by about one third, consistent with the unbound pulse being uncorrelated in phase. The modulation period is 0.104 nm, corresponding to a time separation between the bound pulses of 36.26 ps. This is confirmed by autocorrelation measurement (see the inset of Fig. 7). The autocorrelation trace is best fit with a  $\text{sech}^2$  profile leading to an inferred pulse duration of 100 fs (assuming  $\text{sech}^2$  pulse shape). The average power of 78 mW, which corresponds to energy per pulse of 1.3 nJ (1.75 nJ intra-cavity).

After further decreasing the pumping power to below 1.77 W, one of the bound pulses disappears and the laser supports two unbounded pulses separated by about 20 ns (output power of 67 mW). No modulation is observed on the optical spectrum. For pump powers less than 1.7 W, the laser operates in the single pulse regime with pulse energy exceeding 2 nJ. Mode-locking is lost once the pump power is decreased below 1.6 W.

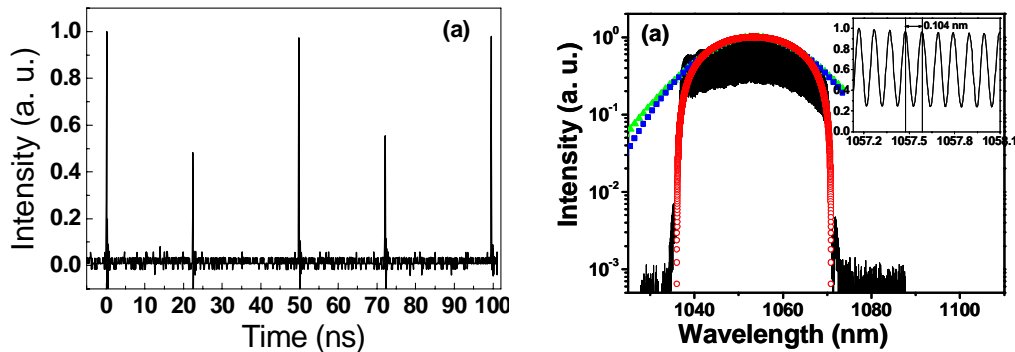


Fig. 6. (a) 5 GHz-oscilloscope trace of a pair of bound pulses and a single pulse. (b) Optical spectrum of co-emission of a pair of bound pulses and a single pulse. The open circles are theoretical fit for a parabolic pulse shape. The closed squares (triangles) are for Gaussian ( $\text{sech}^2$ ) fit and the inset shows a magnified portion of the optical spectrum on a linear scale.



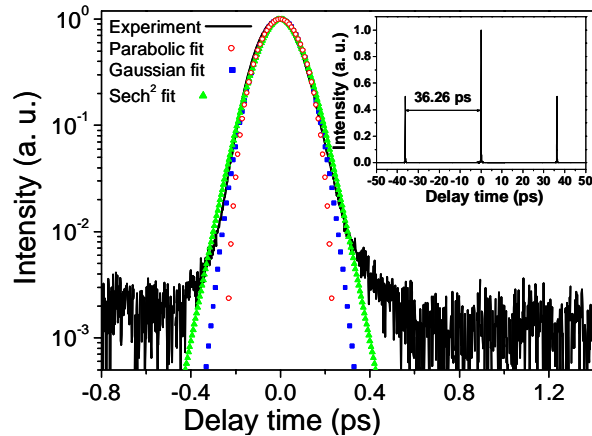


Fig. 7. Central peak of the autocorrelation trace after extra-cavity compression in the case of co-emission of a pair of bounded pulses and a single pulse. The inset shows the complete autocorrelation trace. Pulse duration assuming a sech<sup>2</sup> shape is 100 fs.

#### 4. Conclusion

In conclusion, we report the experimental observation of ultra-short bound states in an ytterbium-doped double-clad fiber laser operating in the self-similar regime. Along with the previously reported results on bound pulse formation in the soliton and the stretched-pulse regimes, these results constitute the observation of the last member of the family of bound pulses; bound pulses exist for all common mode-locking regimes. Therefore, one is led to the significant conclusion that the mechanism underlying the formation of bound pulses is independent of the precise details of the complex interplay between Kerr nonlinearity and dispersion, which dominates pulse shaping. Positively chirped two or three parabolic bound pulses with more than 1.5 nJ energy per pulse are obtained. These pulses are extra-cavity compressed to about 100 fs with a factor of 30, or more. The triplet state demonstrates that the inter-pulse separation is not necessarily constant when more than two pulses are bound, which has important implications for passive harmonic mode-locking operation of fiber lasers. We also report the observation of disassociation of the triplet to a bound doublet and a free pulse, when the effective nonlinearity of the system is decreased via the reduction of pump power. The important feature of these two structures is their zero relative speed which could be attributed to their particular phase relationship that would be 0 or  $+\pi$ . From a practical point of better understanding of the bound pulse formation mechanism may be the key to overcoming the limitation to pulse energy in fiber lasers utilizing the P-APM technique.

#### Acknowledgments

The authors thank Thomas Schreiber and Philippe Grelu for valuable discussions. One of the authors (FOI) acknowledges support from the National Nanotechnology Research Center of Turkey.